

# AN EXPERIMENTAL EVALUATION OF ROBUST GAIN SCHEDULED CONTROLLERS FOR AMB SYSTEM WITH GYROSCOPIC ROTOR

Selim Sivrioglu,<sup>1</sup> Kenzo Nonami<sup>1</sup>

---

## ABSTRACT

This study proposes a new gain scheduled control design approach for Active Magnetic Bearing (AMB) systems. A gyroscopic rotor AMB system is modeled as a linear parameter varying (LPV) plant and controller design is performed using the LPV model of an AMB system. The gain scheduling approach is extended to sliding mode control design. The experiments are carried out using a commercial turbomolecular pump system, and results for gain scheduled controllers are compared with actual PID control results. In the proposed approach, the designed controller has a time varying structure with rotational speed measurements and maintains robust stability as well as good performance even if the rotor has considerable imbalance.

## INTRODUCTION

If an AMB system has an overhang type rotor construction, the gyroscopic couple has considerable influence on the rotor dynamics and increases the instability in the AMB control system. Therefore, to control such systems with PID control is quite difficult especially when the imbalance effect on the rotor increases. One of the most important reasons is that the operating condition of the AMB system is moving with rotational speed, and PID control does not fit the plant operating conditions during control operation because it is designed for a fixed operating condition.

In this study, we treat a gyroscopic AMB system as a linear parameter varying (LPV) plant. Using an LPV plant model of the AMB system, a gain scheduled controller is designed using a linear matrix inequality (LMI) based approach as proposed in (Apkarian and Gahinet, 1995) and (Apkarian, Gahinet and Becker, 1995). The gain-scheduling control design approach is also extended for sliding mode control hyperplane design. We carry out experiment using online scheduling of the designed controller with rotational speed measurements. The experimental results are good even for considerable imbalance on the rotor.

## MODELING OF GYROSCOPIC ROTOR-AMB SYSTEM

In a turbomolecular pump system, the rotor is assumed to be rigid because the flexible modes of the rotor are at very high frequency compared with the operational speed. On the other hand, the rotor has a overhang type construction with blades at the end of the rotor. This structure creates considerable gyroscopic effects on the plant. These effects must be considered in modeling. The equations of motion of the rotor-magnetic bearing system illustrated in Fig.1 are

---

<sup>1</sup>Department of Mechanical Engineering, Chiba University, 1-33 Yayoi-cho, Inage-ku, Chiba 263, Japan.

$$\begin{aligned}
 m\ddot{x}_g &= f_{x_u} + f_{x_b} + m_{un}l\omega_z^2 \cos\alpha \\
 J_r\dot{\beta} &= -J_a\omega_z\dot{\alpha} + L_u f_{x_u} - L_b f_{x_b} \\
 m\ddot{y}_g &= f_{y_u} + f_{y_b} + m_{un}l\omega_z^2 \sin\alpha \\
 J_r\dot{\alpha} &= J_a\omega_z\dot{\beta} - L_u f_{y_u} + L_b f_{y_b}
 \end{aligned}
 \tag{1}$$

Table 1 shows the parameter values of the system. Control forces produced by upper side AMB can be expressed by

$$\begin{aligned}
 f_{x_u} &= 2K_{du}x_g + 2L_uK_{du}\beta + 2K_{iu}i_{x_u} \\
 f_{y_u} &= 2K_{du}y_g - 2L_uK_{du}\alpha + 2K_{iu}i_{y_u}
 \end{aligned}
 \tag{2}$$

while the lower side forces produced by the permanent magnetic bearing (PMB) are

$$\begin{aligned}
 f_{x_b} &= -2C_b\dot{x}_g + 2C_bL_b\dot{\beta} - 2K_bx_g + 2K_bL_b\beta \\
 f_{y_b} &= -2C_b\dot{y}_g - 2C_bL_b\dot{\alpha} - 2K_by_g - 2K_bL_b\alpha
 \end{aligned}
 \tag{3}$$

The equations of motion of the rotor-bearing system can be written in more compactly as

$$M\ddot{z}_f + (G_c + G_j)\dot{z}_f + Kz_f = Fu + Ew
 \tag{4}$$

where  $M, G_c, G_j$  and  $K$  are the mass matrix, the damping matrix, the gyroscopic matrix and the stiffness matrix, respectively.  $F$  and  $E$  describe the control input and the disturbance input locations, respectively. The vector  $z_f$  represents the displacement variables of the rotor with respect to the center of gravity, measured in the fixed coordinate system,

$$z_f = [x_g \quad \beta \quad y_g \quad \alpha]^T
 \tag{5}$$

The gyroscopic effects are characterized by a skew-symmetric matrix  $G_j = -G_j^T$ , which depends linearly on the rotational speed  $\omega_z$ . The unbalance effects vary as the square of the rotational speed  $\omega_z$ . The linearization of the unbalance effect is described in (Sivrioglu and Nonami, 1996). Finally, the LPV state-space representation of this system takes the form

$$\begin{aligned}
 \dot{x} &= A(\omega_z)x + B_2u + B_1(\omega_z)w \\
 y &= Cx
 \end{aligned}
 \tag{6}$$

where  $x$  is the state vector,  $y$  is the measured output vector and  $u$  is the control input vector. The system matrices are

$$A(\omega_z) = \begin{bmatrix} 0 & I \\ -M^{-1}K & -M^{-1}(G_c + G_j(\omega_z)) \end{bmatrix}, \quad B_1(\omega_z) = \begin{bmatrix} 0 \\ M^{-1}E(\omega_z) \end{bmatrix}, \quad B_2 = \begin{bmatrix} 0 \\ M^{-1}F \end{bmatrix}
 \tag{7}$$

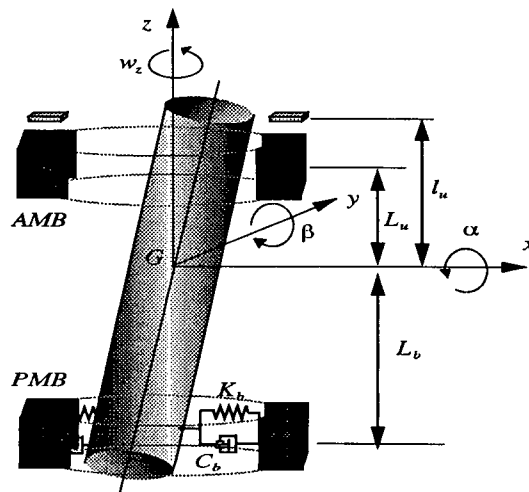


Fig.1 Model of the rotor-active bearing system

Table 1 Parameter values of the AMB system

Parameter	Symbol	Unit
Mass of the rotor	$m$	kg
Moment of inertia around radial axis	$J_r$	$kgm^2$
Polar moment of inertia	$J_a$	$kgm^2$
Distance of the upper AMB to the CG	$L_u$	m
Distance of the below PMB to the CG	$L_b$	m
Distance of the sensor to the CG	$l_u$	m
Linearized force/current factor	$K_{iu}$	N/A
Linearized force/displacement factor	$K_{du}$	N/m
Stiffness coefficient of the PMB	$K_b$	N/m
Damping coefficient of the PMB	$C_b$	kg/s
Unbalance mass	$m_{un}$	kg
Distance of the unbalance mass from center	$l$	m

### GAIN-SCHEDULED $H_\infty$ CONTROL DESIGN

The theoretical formulation of the gain-scheduled control design approach is proposed in (Apkarian and Gahinet, 1995) and (Apkarian, Gahinet and Becker, 1995). The recent studies (Apkarian and Adams, 1997) and (Tsiotras and Knopse, 1997) deal with the gain scheduled control design more extensively.

In this study, the turbomolecular pump as a control object speeds up from 0 to 48000 rpm in 3 minutes, and speeds down in breaking mode in the same amount of time. Parameter dependence range of the plant due to rotational speed is

$$\omega_z(t) \in [\underline{\omega}_z, \bar{\omega}_z] = [0 \ 2\pi 800] \quad (8)$$

Controller design reflects the parameter variation in a polytopic plant structure. The parameter dependence of the plant in the polytopic form is given by

$$P(\alpha_1, \alpha_2) = \begin{bmatrix} 0 & [0 \ B_2] \\ C & 0 \end{bmatrix} + \alpha_1 \begin{bmatrix} A(\underline{\omega}_z) & [B_1(\underline{\omega}_z) \ 0] \\ 0 & 0 \end{bmatrix} + \alpha_2 \begin{bmatrix} A(\bar{\omega}_z) & [B_1(\bar{\omega}_z) \ 0] \\ 0 & 0 \end{bmatrix} \quad (9)$$

The parameters  $\alpha_1$  and  $\alpha_2$  are obtained by the following convex relation

$$\sum_{i=1}^2 \alpha_i = \underbrace{\frac{\bar{\omega}_z - \omega_z(t)}{\bar{\omega}_z - \underline{\omega}_z}}_{\alpha_1} + \underbrace{\frac{\omega_z(t) - \underline{\omega}_z}{\bar{\omega}_z - \underline{\omega}_z}}_{\alpha_2} = 1, \quad \alpha_i \geq 0 \quad (10)$$

In this control system, there are two basic design requirements. First, maximum gain of the gain scheduled controller should not be higher than the PID controller gain because power amplifiers of the control system are designed for PID. Second, the closed-loop frequency response should be wide band because the operational speed of the plant is quite high. These design requirements specify two weighting functions for performance improvements in the control system. For each direction of the rotor, the frequency shaping filters are described by

$$W_1(s) = \frac{k_1(s+q)}{(s+k_2p)}, \quad W_2(s) = \frac{k_2p}{(s+k_2p)} \quad (11)$$

where  $p$  is the unstable pole of the plant and  $q$ ,  $k_1$ ,  $k_2$  are specified in experiments. Here, the smaller  $k_1$  values increase controller gain and reduce robust stability.  $k_2$  is related to frequency band of the closed-loop system. The frequency shaping filters for  $q = 1$ ,  $k_1 = 0.1$  and  $k_2 = 5$  values are used for controller design. Using the frequency shaping filters, the parameter dependent form of the augmented plant can be given by

$$G(\omega_z) = \begin{bmatrix} A(\omega_z) & B_1(\omega_z) & B_2 \\ C_1 & D_{11} & D_{12} \\ C_2 & D_{21} & D_{22} \end{bmatrix} \quad (12)$$

Finally, using the parameter-dependent augmented plant, the gain-scheduled controller is computed using the LMI Control Toolbox (Gahinet et.al., 1995). The controller has the form of

$$K(\omega_z) = \begin{bmatrix} A_K(\omega_z) & B_K(\omega_z) \\ C_K(\omega_z) & D_K(\omega_z) \end{bmatrix} \quad (13)$$

To perform the scheduling of the controller with rotational speed measurement  $\omega_z(t)$ , the controller state-space matrices should be computed at time  $t$  as the convex combination of the following control structure

$$\begin{bmatrix} A_K(t) & B_K(t) \\ C_K(t) & D_K(t) \end{bmatrix} = \frac{\bar{\omega}_z - \omega_z(t)}{\bar{\omega}_z - \underline{\omega}_z} \begin{bmatrix} A_K(\underline{\omega}_z) & B_K(\underline{\omega}_z) \\ C_K(\underline{\omega}_z) & D_K(\underline{\omega}_z) \end{bmatrix} + \frac{\omega_z(t) - \underline{\omega}_z}{\bar{\omega}_z - \underline{\omega}_z} \begin{bmatrix} A_K(\bar{\omega}_z) & B_K(\bar{\omega}_z) \\ C_K(\bar{\omega}_z) & D_K(\bar{\omega}_z) \end{bmatrix} \quad (14)$$

Here letting  $\omega_z(t) = \underline{\omega}_z$ , one can obtain a controller  $K^{(1)}$  which is used for levitation of the rotor ( $\omega_z = 0$ ). Also letting  $\omega_z(t) = \bar{\omega}_z$ , gives the operational controller  $K^{(2)}$  ( $\omega_z = 48000$  rpm). Each controller is called the vertex controller for gain scheduling. The gain-scheduled controller frequency responses with rotational speed variation are shown in Fig.2. As can be seen in this figure, the controller has dynamics with respect to parameter variation.

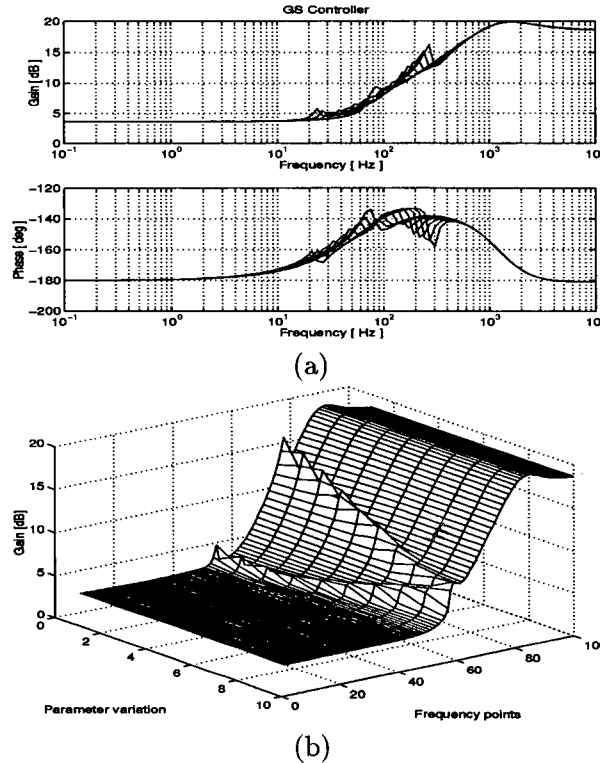


Fig.2 Bode plot of the GS controller (a) 2D (b) 3D

MIMO CONTROL STRUCTURE

The gain-scheduled controller designed here is a centralized MIMO controller. Thus, the controller has two inputs and two outputs and the controller transfer matrix has four transfer functions as follows:

$$K_T(\omega_z) = \begin{bmatrix} K_{xx}(\omega_z) & K_{xy}(\omega_z) \\ K_{yx}(\omega_z) & K_{yy}(\omega_z) \end{bmatrix} \quad (15)$$

Since the gain-scheduled controller implementation is a digital signal processor(DSP) based application, the continuous time controller should be converted to the discrete time controller. Each vertex controller  $K^{(1)}$  and  $K^{(2)}$  in Eq.(14), are discretized using bilinear (Tustin) transformation.

The frequency responses of discrete time controllers  $K_{xx}(\omega_z)$  and  $K_{xy}(\omega_z)$  are given in Figs.3(a)-(b). For a successful levitation of the rotor using the centralized gain-scheduled controller, gain of the cross controllers  $K_{xy}(\omega_z)$  and  $K_{yx}(\omega_z)$  must be below -40 dB at  $\omega_z = 0$ . This condition is necessary for obtaining equal control input for each direction. Actually, the cross controller dynamics provide an effective control dynamics in rotation.

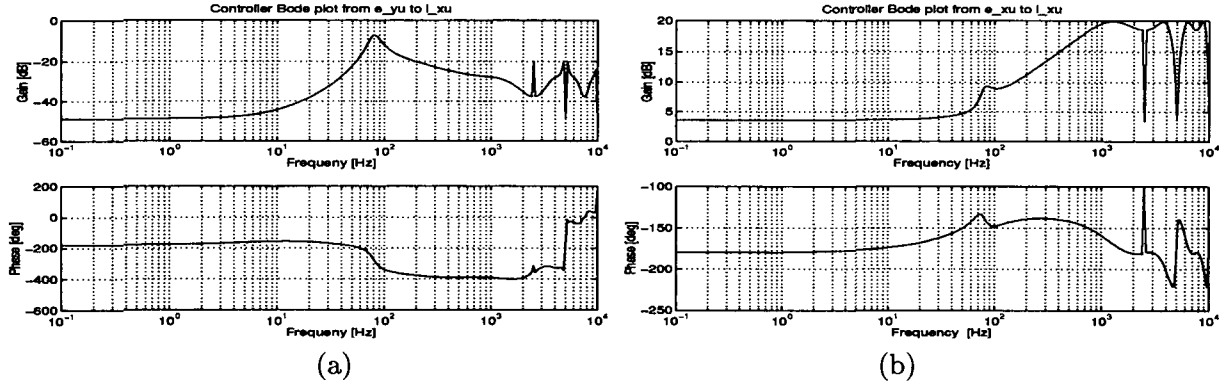


Fig.3 Bode plot of the discretized GS controller at  $\omega_z = 0$  (a)  $K_{xy}$ , (b)  $K_{xx}$

**SLIDING MODE CONTROL DESIGN**

Sliding mode control uses a nonlinear control input which yields a more suitable control structure particularly if a plant itself is nonlinear. The aim of this section is to design a scheduled sliding mode control using the frequency shaped sliding mode control approach proposed in (Young and Ozguner, 1993). Basically, this approach involves a compensator design for producing an equivalent control input for the sliding mode as proposed in (Nonami, Nishimura and Tian, 1996).

**SCHEDULED HYPERPLANE DESIGN**

The extension of the frequency shaped sliding mode control to LPV plants is proposed in (Sivrioglu and Nonami, 1998). Consider the state space representation of the LPV plant given in Eq.(6)

$$\begin{aligned} \dot{x} &= A(\omega_z)x + B_2u + B_1(\omega_z)w \\ y &= Cx \end{aligned} \tag{16}$$

To retain the parameter dependence of the original plant and give integral action to the control input, a low-pass pre-filter is chosen as follows:

$$\begin{aligned} \dot{x}_f &= A_f x_f + B_f u \\ y_f &= C_f x_f \end{aligned} \tag{17}$$

Combining the state space model of the plant with the above filter, yields augmented structure as a transformed system for sliding mode control design as

$$\begin{aligned} \begin{bmatrix} \dot{x} \\ \dot{x}_f \end{bmatrix} &= \begin{bmatrix} A(\omega_z) & B_2 C_f \\ 0 & A_f \end{bmatrix} \begin{bmatrix} x \\ x_f \end{bmatrix} + \begin{bmatrix} 0 \\ B_f \end{bmatrix} u + \begin{bmatrix} B_1(\omega_z) \\ 0 \end{bmatrix} w \\ y &= \begin{bmatrix} C & 0 \end{bmatrix} \begin{bmatrix} x \\ x_f \end{bmatrix} \end{aligned} \tag{18}$$

or

$$\begin{aligned} \begin{bmatrix} \dot{x}_1 \\ \dot{x}_2 \end{bmatrix} &= \begin{bmatrix} A_{11}(\omega_z) & A_{12} \\ A_{21} & A_{22} \end{bmatrix} \begin{bmatrix} x_1 \\ x_2 \end{bmatrix} + \begin{bmatrix} 0 \\ B \end{bmatrix} u + \begin{bmatrix} B_1(\omega_z) \\ 0 \end{bmatrix} w \\ y &= \begin{bmatrix} C & 0 \end{bmatrix} \begin{bmatrix} x_1 \\ x_2 \end{bmatrix} \end{aligned} \tag{19}$$

Now, a switching surface for this control system is offered as

$$\Phi = S(x_1) + x_2 \quad (20)$$

where the switching function  $S(x_1)$  is a linear operator of  $x_1$ . The proposed switching surface  $\Phi$  will have some dynamics as compared to a conventional one in terms of the compensator dynamics. If measurements of the time-varying parameter  $\omega_z$  are available in real time, then the compensator will have parameter dependence described by

$$\begin{aligned} \dot{z} &= F(\omega_z)z + G(\omega_z)e \\ S(x_1) &= -H(\omega_z)z - L(\omega_z)e \end{aligned} \quad (21)$$

where  $z$  is the state vector of compensator. Specifically, the control system is considered as a servo-type and the error signal is defined by

$$e = r - Cx_1 \quad (22)$$

where  $r$  is the reference signal. It is evident that Eq.(21) is a state-space representation of the gain scheduled controller given in Eq.(13).

#### VSS CONTROLLER DESIGN

We seek a Lyapunov function such that

$$V = \frac{1}{2} \Phi \Phi \quad (23)$$

The following condition should be satisfied for existence of a sliding mode and stabilization of the closed-loop system

$$\dot{V} = \Phi \dot{\Phi} < 0 \quad (24)$$

For simplicity, the compensator is assumed strictly proper,  $L(\omega_z) = 0$ . For a single parameter case such as  $\omega_z$ , the derivative of the hyperplane is obtained by

$$\begin{aligned} \Phi &= (\alpha_1 H_1 + \alpha_2 H_2)z + x_2 \\ \dot{\Phi} &\equiv \frac{d\Phi(z, x_2, \alpha_1, \alpha_2)}{dt} \\ &= -(\alpha_1 H_1 + \alpha_2 H_2)\dot{z} + \dot{x}_2 - (\dot{\alpha}_1 H_1 + \dot{\alpha}_2 H_2)z \\ &= -\left(\sum_{i=1}^2 \alpha_i H_i \dot{z} + \dot{\alpha}_i H_i z\right) + \dot{x}_2 \end{aligned} \quad (25)$$

where  $\alpha_1$  and  $\alpha_2$  are given in Eq.(10). The fixed matrices  $H_1$  and  $H_2$  are obtained by using extremal values of the rotational speed. From the Eq.(24),

$$\begin{aligned} \dot{V} &= \Phi \dot{\Phi} \\ &= \Phi \left(-\left(\sum_{i=1}^2 \alpha_i H_i \dot{z} + \dot{\alpha}_i H_i z\right) + \dot{x}_2\right) \\ &= \Phi \left\{ \left(-\sum_{i=1}^2 \alpha_i H_i F_i + \dot{\alpha}_i H_i\right)z + \left[\left(\sum_{i=1}^2 \alpha_i H_i G_i C\right) + A_{21}\right]x_1 + A_{22}x_2 + Bu \right\} \\ &= \Phi B(u - u_l) \end{aligned} \quad (26)$$

where the equivalent control input  $u_l$  is obtained by imposing the condition  $\Phi = \dot{\Phi} = 0$

$$u_l = -B^{-1} \left[ \left(-\sum_{i=1}^2 \alpha_i H_i F_i + \dot{\alpha}_i H_i\right)z + \left[\left(\sum_{i=1}^2 \alpha_i H_i G_i C\right) + A_{21}\right]x_1 + A_{22}x_2 \right] \quad (27)$$

The condition of Eq.(24) becomes

$$\dot{V} = \Phi B(u - u_l) < 0 \tag{28}$$

The control input  $u$  which satisfies the condition of Eq.(28) can be chosen as

$$u = \begin{cases} u_l - u_n & B\Phi > 0 \\ u_l + u_n & B\Phi < 0 \end{cases} \tag{29}$$

A nonlinear control input  $u_n$  is given by

$$u_n = \epsilon_s \frac{B\Phi}{\|B\Phi\| + \eta_s} \tag{30}$$

where  $\epsilon_s > 0$  and  $\eta_s > 0$  are selected as 0.1 and 0.01, respectively.  $\eta_s$  is used for a smooth discontinuous control input.  $\epsilon_s$  is chosen from experimental considerations. For slow parameter variations, the derivative  $\dot{\alpha}$  of the parameter  $\alpha$  becomes very small, and the  $\dot{\alpha}_i H_i z$  term can be neglected.

### PID CONTROL

A brief introduction of the PID control is given for comparing the gain-scheduled control results with PID results. In an actual case, the plant is controlled by analog PID controllers. Two identical PID controllers have been installed in a decentralized structure. The frequency response of the PID controller is given in Fig.4.

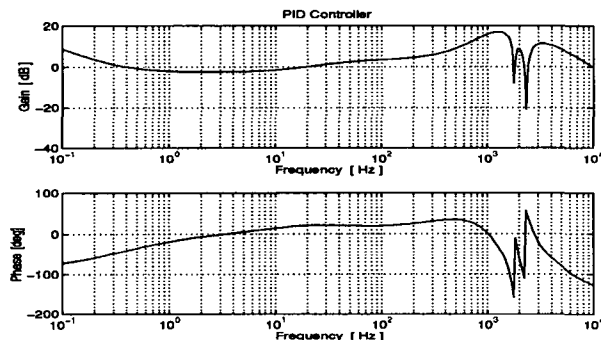


Fig.4 Frequency response of the PID controller

## IMPLEMENTATION OF ROBUST CONTROLLERS

### GAIN SCHEDULED $H_\infty$ CONTROL

The implementation of the gain scheduled controllers on a DSP has special importance because of its time varying structure. The discretization of gain scheduled controllers is defined in (Apkarian, 1997). A discrete state-space representation of the continuous time controller given in Eq.(14) is obtained for real time implementation. The C-source code of the gain scheduled controller is generated using the C language commands included in the DSP library. The discrete state space representation of the gain scheduled controller is given by

$$\begin{aligned} x_{k+1} &= [(1 - \alpha_k)A_d^{(1)} + \alpha_k A_d^{(2)}]x_k + [(1 - \alpha_k)B_d^{(1)} + \alpha_k B_d^{(2)}]y_k \\ u_k &= [(1 - \alpha_k)C_d^{(1)} + \alpha_k C_d^{(2)}]x_k + [(1 - \alpha_k)D_d^{(1)} + \alpha_k D_d^{(2)}]y_k \end{aligned} \tag{31}$$

where  $\alpha_k = \frac{\omega_{zk}}{\bar{\omega}_z}$  and  $A_d^{(i)}, B_d^{(i)}, C_d^{(i)}, D_d^{(i)}$ , ( $i=1,2$ ) are the discretized vertex controller matrices.

## SCHEDULED SLIDING MODE CONTROL

The sliding mode controller is obtained using the VSS controller structure. The computation of controller output is realized by using the following steps.

$$\begin{aligned}
 z_{k+1} &= [(1 - \alpha_k)F_d^{(1)} + \alpha_k F_d^{(2)}]x_k + [(1 - \alpha_k)G_d^{(1)} + \alpha_k G_d^{(2)}]y_k \\
 S_k &= [(1 - \alpha_k)H_d^{(1)} + \alpha_k H_d^{(2)}]x_k \\
 \Phi_k &= B_{w_k}(S_k + x_{w_k}) \\
 u_{n_k} &= \epsilon_s \frac{B_{w_k} \Phi_k}{\|B_{w_k} \Phi_k\| + \eta_s} \\
 u_{l_k} &= -B_{w_k}^{-1}[-(1 - \alpha_k)H_d^{(1)} + \alpha_k H_d^{(2)}]z_{k+1} + x_{w_{k+1}} \\
 u_{t_k} &= u_{l_k} + u_{n_k} \\
 x_{w_{k+1}} &= A_{w_k}x_{w_k} + B_{w_k}u_{t_k} \\
 u_k &= C_{w_k}x_{w_k}
 \end{aligned} \tag{32}$$

## EXPERIMENTAL RESULTS

The configuration of the experimental setup is schematically shown in Fig.5. An actual turbo-molecular pump is used for the experiment. The gain scheduled  $H_\infty$  controller and sliding mode controller are installed on the DSP (TMS320C30) and experiments are carried out. The sampling time of the controllers are 0.2 msec (sampling frequency 5KHz). Two displacements measured by two position sensors in the  $x$  and  $y$  directions and the rotational speed signal  $\omega_z$  are transmitted to the DSP through A/D converters. Control inputs are supplied to electromagnets through D/A converters and power amplifiers. The rotational speed signal  $\omega_z$  is measured with a pulse modulation of 0.2 msec between 0 to 2.5 V amplitude. In addition, the bias current and nominal gap are 0.38 A and 0.275 mm, respectively.

In rotating systems, there is an unpredictable disturbance effect synchronizing rotating speed owing to mass imbalances of the rotor. As an industrial demand, the control objective is to maintain stability and robustness even if the rotor has some imbalance effect. For this reason, the controllers are tested by mounting some unbalance mass on the rotor. The PID and gain-scheduled controllers performance are evaluated for two different cases. The first case is the nominal operation of the plant. The second one is the unbalance case. The sliding mode controller is tested only for the unbalance case.

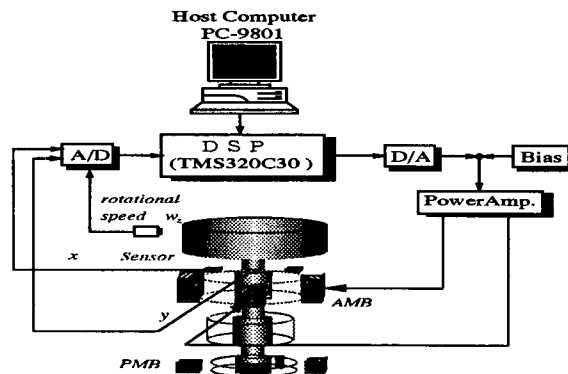


Fig.5 Configuration of the experimental setup

## NOMINAL CASE

For critical speed range, the orbits of the rotor's central axis for the nominal case with gain-scheduled control and PID control are displayed in Fig.6 and Fig.7, respectively. It can be observed that the critical speed passing with gain-scheduled control is faster than that of PID control. The high speed rotation range is nearly the same for gain scheduled control and PID control as shown

in Fig.8 and Fig.9, respectively. In all measured results, synchronization is satisfactory even if the rotor passes the critical speeds.

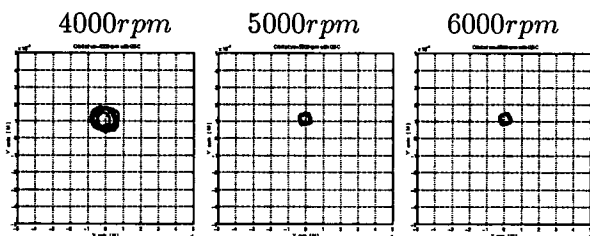


Fig.6 Orbits with GSC for nominal case  
(Axes wide  $\pm 50\mu\text{m}$ )

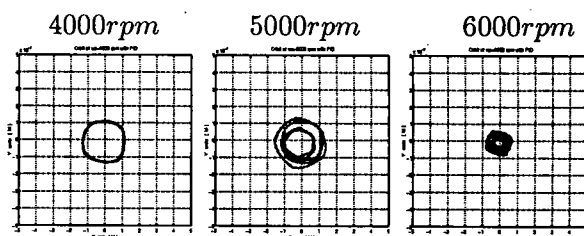


Fig.7 Orbits with PID for nominal case  
(Axes wide  $\pm 50\mu\text{m}$ )

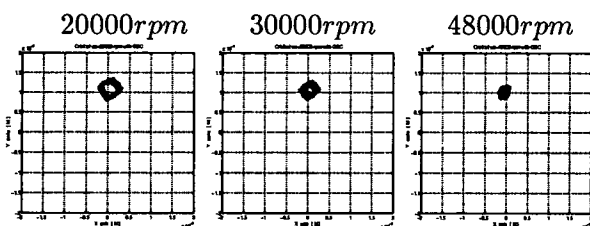


Fig.8 Orbits with GSC for nominal case  
(Axes wide  $\pm 20\mu\text{m}$ )

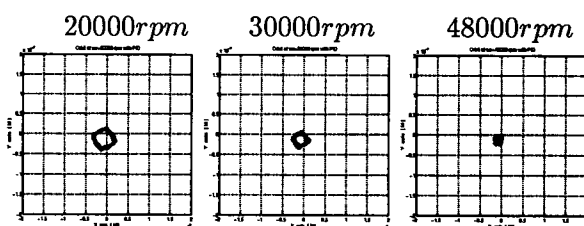


Fig.9 Orbits with PID for nominal case  
(Axes wide  $\pm 20\mu\text{m}$ )

UNBALANCE CASE

In this case, the unbalance mass mounted on the rotor is 12 g mm. The orbits for the critical speed region are given in Figs.10-12. These results are quite interesting and explain how the scheduling of the controller is effective during critical speed passing. Since the rotor has a very complicated dynamics under the gyroscopic and imbalance effects, increasing the controller gain in critical speed region does not provide a successful critical speed passing. In our observations, the behavior of PID controller is to increase the controller gain due to this rotor dynamics. On the other hand, the lower side of the rotor has no active control, and large control forces at the upper side cause vibration at the lower side. What is needed is a kind of control dynamics which stabilizes the system within a given tolerance of orbits. As can be seen in Fig.2, the gain-scheduled control dynamics satisfies this condition perfectly. The increase and then the decrease of the controller gain in the critical speed region provides a kind of relaxation to the rotor, with the increase of diameter of orbits within allowed tolerance. This dynamics maintains a soft critical speed passing as shown in Figs.10-11. Although the diameter of the orbits with PID control is small until 6000 rpm as shown in Fig.12, the lower side of the rotor is in touch down position and above 15000 rpm it is impossible to run the plant due to vibration. The plant safely speeds up to 48000 rpm when using the gain scheduled controller. We could not rotate the rotor at 48000 rpm using sliding mode controller because of instability of the obtained discrete controller above 30000 rpm. The reason was that the transformation method used for discretization was a zero-order hold for the sake of obtaining a strictly proper controller.

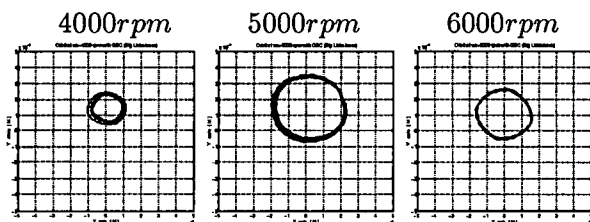


Fig.10 Orbits with GSC for unbalance case  
(Axes wide  $50\mu\text{m}$ )

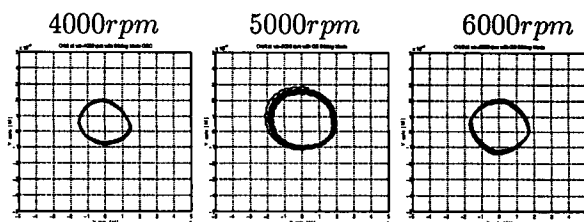
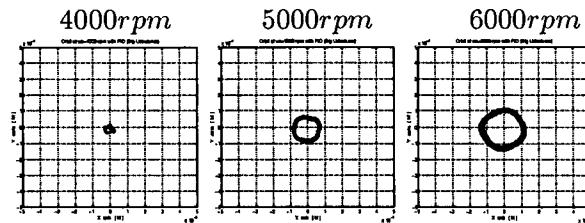
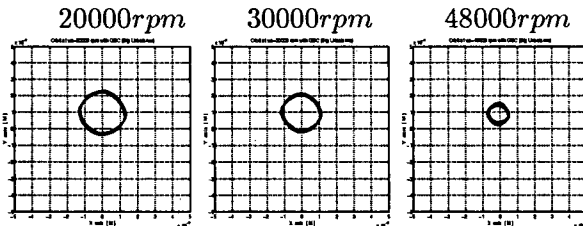
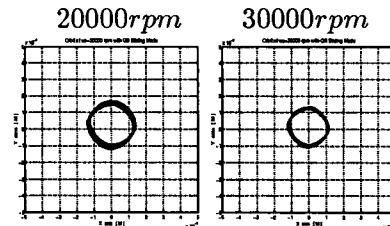


Fig.11 Orbits with SMC for unbalance case  
(Axes wide  $50\mu\text{m}$ )

Fig.12 Orbits with PID for unbalance case (Axes wide  $\pm 50\mu\text{m}$ )Fig.13 Orbits with GSC for unbalance case  
(Axes  $50\mu\text{m}$ )Fig.14 Orbits with SMC for unbalance case  
(Axes  $50\mu\text{m}$ )

## CONCLUSIONS

In this study, a novel idea for robust gain scheduled control design is applied to an AMB system with gyroscopic rotor. The gain scheduling approach is also extended to scheduled sliding mode control design. Experiments have been carried out for an online scheduling of the controller with rotational speed measurements. The gain scheduled controller and scheduled sliding mode controller satisfy the strong stabilization requirement, even for the considerable unbalance case. These results were compared with PID control both in nominal case and considerable unbalance case on the rotor.

## REFERENCES

- Apkarian P., P. Gahinet. 1995. "A Convex Characterization of Gain Scheduled  $H_\infty$  Controllers," IEEE. Trans. on Automatic Control, vol.40, pp.853-863.
- Apkarian P., P. Gahinet, G. Becker. 1995. "Self-scheduled  $H_\infty$  Control of Linear Parameter-varying Systems: a Design Example," Automatica, vol.31-9, pp.1251-1261.
- Apkarian P., and P.J. Adams. 1998. "Advanced Gain-Scheduling Techniques for Uncertain Systems", IEEE Transactions on Control Systems Technology, vol.6, no.1, pp. 21-32.
- Apkarian P. 1997. "On the Discretization of LMI-Synthesized Linear Parameter-Varying Controllers," Automatica.
- Gahinet P., A. Nemirovski, A.J. Laub, M. Chilali. 1995. "LMI Control Toolbox, For Use with MATLAB."
- Nonami K., H. Nishimura, H. Tian. 1996. " $H_\infty/\mu$  Control-based Frequency-shaped Sliding Mode Control for Flexible Structures," JSME International Journal, Series C, vol.39, No.3, pp. 493-501.
- Sivrioglu S., K. Nonami. 1998. "Sliding Mode Control with Time Varying Hyperplane for AMB Systems," IEEE/ASME Trans. on Mechatronics, vo.3, no.1, pp. 51-59.
- Sivrioglu, S., K. Nonami. 1996. "LMI Based Gain Scheduled  $H_\infty$  Controller Design For AMB Systems Under Gyroscopic and Unbalance Disturbance Effect," Proceedings of 5th ISMB, pp. 191-196.
- Young D., U. Ozguner. 1993. "Frequency Shaping Compensator Design for Sliding Mode Control," Int. Journal of Control, vol.57, No.5, pp.1005.